Analysis and Design of Four-Plate Capacitive Wireless Power Transfer System for Undersea Applications

Lei Yang, *Member, IEEE*, Yuanqi Zhang, Xiaojie Li, Jiale Jian, Zhe Wang, Jingjing Huang, *Member, IEEE*, Li Ma, and Xiangqian Tong

***Abstract*—This paper presents a four-plate undersea capacitive wireless power transfer (CPT) system for underwater applications such as autonomous underwater vehicles (AUVs). Generally, a CPT system transfers the power based on electric fields. The complex resonant compensation networks are used to make the CPT system work in the resonant condition. The resonant voltage is always very high. It will be a big challenge to the human safety. In this paper, a virtual electrons periodic reciprocating flow theory is proposed for the CPT system. In one switching cycle, the electrons firstly flow in the forward direction through the forward path and then flow in the inverse direction through the inverse path. The CPT system has been deeply studied with the vacuum dielectric or the air dielectric. However, for the CPT system, there are few papers to show the underwater application. In this paper, an undersea four-plate CPT system is designed and studied in the underwater condition. The two coupling capacitors and other elements of the CPT system could build a closed-loop path. A small value inductor is adapted as a resonant compensation network for the four-plate CPT system. The DC voltage is inverted to the AC voltage in the primary side with the single-phase full-bridge inverter. The resonant voltage is rectified to the DC voltage in the secondary side with the single-phase full-bridge diode rectifier. A 100 W power level CPT system is constructed to verify the theory analysis and the calculation. The theory analysis is verified by the simulated and experimental results. The stable output voltage and load power are achieved in this paper.**

***Index Terms*—Wireless power transfer system, capacitive, underwater applications, autonomous underwater vehicles (AUVs).**

Manuscript received May 24, 2021; revised June 29, 2021; accepted August 24, 2021. date of publication September 25, 2021; date of current version September 18, 2021.

This work was supported by the National Natural Science Foundation of China under grant no.52107205, China Postdoctoral Science Foundation under grant no.2018M643700, Scientific Research Project of Education Department of Shaanxi Province under grant no.18JS080, Postdoctoral Research Program of Shaanxi Province under grant no. 2018BSHYDZZ28 and Basic Research Project of Natural Science of Shaanxi Province under grant no. 2020JQ-623.*(Corresponding Author: Lei Yang)*

Lei Yang, Yuanqi Zhang, Xiaojie Li, Jiale Jian, Zhe Wang, Li Ma and Xiangqian Tong are with School of Electrical Enginerring, Xi'an Technology of University, Xi'an, 710048, China. (e-mail: yangeli0930@ xaut.edu.cn).

Jingjing Huang is with the School of Electronic and Information Engineering, Xi'an Jiaotong University, Xi'an 710049, China (e-mail: hjj7759@163.com)

Digital Object Identifier 10.30941/CESTEMS.2021.00024

I. INTRODUCTION

WIRELESS power transfer (WPT) system is a technology that can deliver the power without the physical contact. Several methods of wireless power transfer technology have been introduced including inductive coupling through magnetic fields, capacitive coupling through electric fields, laser-based optical power transmission and far-field RF microwave energy transmission. Inductive wireless power transfer (IPT) utilizes non-radiative magnetic fields with the kHz to MHz range to realize the wireless power transfer function. The inductive coupler is adapted to generate the magnetic fields. IPT system has been widely used for underwater equipment [1]-[6], implantable medical devices [7]-[10], mobile devices [11]-[15], electrical vehicles (EVs) [16]-[20], or drone-in-flight [21]. IPT technologies could provide the benefits such as high efficiency, galvanic isolation, and high reliability especially in hostile environments [22].

In the underwater condition, underwater inductive wireless power transfer (UIPT) system should take care the eddy current loss which is generated by the conductive water as shown in Fig.1. The mutual inductance of UIPT system will change with the variable relative magnetic permeability. The relative magnetic permeability of water will vary with the temperature and salinity. For the UIPT system, it suffers from the large leakage magnetic fields. What's more, the UIPT system is sensitive to the presence of metal material nearby. It will generate heat with the redundant power loss.

Compared to the IPT system, the capacitive wireless power transfer (CPT) system adapts very high-frequency (MHz) electric fields to deliver the power from the transmitter to the

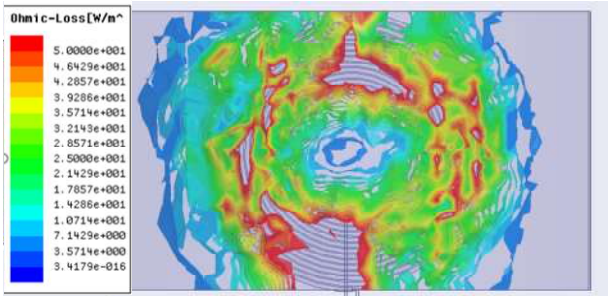

Fig.1. Eddy current loss of IPT system in marine environment (simulated by Ansys Maxwell with 5 A current, 60 mm distance, 100 mm diameter of coil, and the temperature 25℃).

receiver [23]. The transmitter and receiver are built by the meatal plates which are called capacitive coupler. Two coupling capacitors provide a power flow from the power source to the load. The CPT system is usually used for the low power applications. Recently, several kilowatts power level CPT topologies are proposed which could transfer the power with the large distance between the transmitter and the receiver [24]-[27]. The CPT technology has been highly developed in recent years. This technology could also be adapted for the electrical ship and all-electric aircraft.

There are different kinds of coupling capacitor structures for different kinds of CPT systems as shown in Fig.2. The general coupling structure is the four metal plates topology. The transmitter side is consisted by two metal plates (P_1 and P_2) and the receiver side is consisted by two metal plates (P_3 and P_4) as shown in [23] and [25]. These four metal plates build the two coupling capacitor units. The size of the transmitter metal plates could be same to the receiver metal plates as shown in Fig.2 (a). It can be seen from Fig.2 (c), the transmitter metal plates are designed larger than the receiver metal plates to reduce the electric field radiation. In [24], for dynamical wireless power transfer application such as the electric vehicle battery charging, the transmitter metal plates should be long enough to provide the stable power to the receiver metal plates as shown in Fig. 2 (b). In order to prevent electric field emissions to the surrounding environment, paper [26] proposes a six-plate capacitive coupler for large air-gap wireless power transfer application as shown in Fig.2 (d). A combination of the IPT topology and the CPT topology is proposed in [27]. The coupling structure is shown as Fig. 2 (e). As shown in Fig.2 (f), in order to improve the power transfer level, the four transmitter metal plates CPT structure is proposed in [28].

It should figure out that most of the CPT systems are used for air dielectric. There are few papers to show the undersea CPT system. The permittivity of the seawater is about 81 times larger than the permittivity of the free space. With the seawater medium, the power transfer capacity of the CPT system could be highly improved at the same distance between the transmitter and the receiver of the CPT system with the air medium. Compared to the IPT system, the power of the CPT system is delivered through the electric fields. The advantages

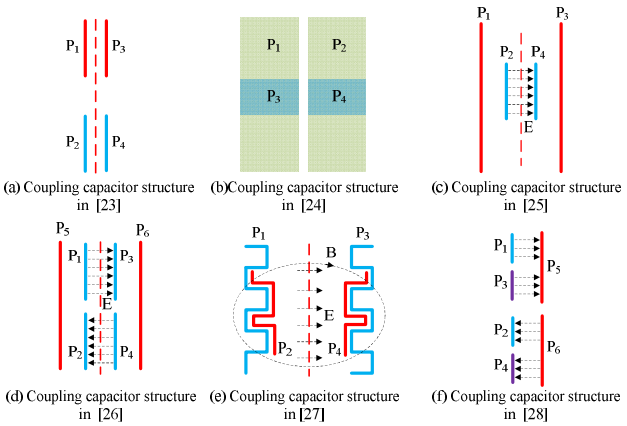

Fig.2.Coupling capacitor structure.

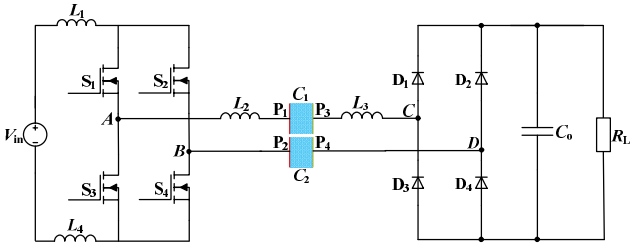

Fig.3. Topology of four-plate CPT system.

of the undersea CPT applications are the low cost and no eddy-current loss with nearby metals. An underwater capacitive wireless power transfer (UCPT) system is proposed in [29] for operation in freshwater. The 91.3% power transfer efficiency is achieved at distance of 20 mm. The capacity of high power UCPT system for electrical ship has been investigated in [30]. The power level reaches 226.9 W across the distance 500 mm with 60.2% efficiency. What's more, it shows that the mathematical theory power capacity of the UCPT system could be as high as MW level. A bidirectional underwater capacitive wireless power transfer (BD-UCPT) has been proposed in [31] and [32] for AUVs' battery charging applications. A 100 W experimental BD-UCPT is built and tested. The power of proposed BD-UCPT system could flow bidirectionally.

Based on aforementioned discussion, in order to extend the CPT system application for the undersea condition, this paper proposes a four-plate CPT system which based on the virtual electrons periodic reciprocating flow theory for the undersea application. The resonant compensation network is only one inductor. The dielectric between the four metal plates is seawater. The electric fields and the power transfer capacity are presented in this paper. The rest of paper is organized as follows: the topology of the four-plate CPT system is shown in Section II. Section III provides the theory analysis of the virtual electrons periodic reciprocating flow theory for the four-plate CPT system. The simulated and experimental verification is shown in Section IV. The conclusions and discussions are drawn in Section V.

II. Topology Model

The four-plate CPT system adapted in this paper is presented as Fig.3. Two inductors (L_2 and L_3) are respectively connected to the coupling capacitor (C_1 which is built by plates P_1 and P_3 and C_2 which is built by plates P_2 and P_4) in serial. Another two inductors (L_1 and L_4) are injected in the charging path of the power source which could reduce the spikes of the input current. The dielectric between the four plates is the seawater. The salinity of the seawater is about 35‰. The power is transferred through the electronic fields with the LC network. The LC network is consisted of the resonant inductor and the coupling capacitor. There are two coupling capacitors which are respectively connected to the full-bridge inverter and the full-bridge diode rectifier. The top coupling capacitor C_1 is built by the metal plates P_1 and P_3. The bottom coupling capacitor C_2 is built by the metal plates P_2 and P_4. The equivalent operation states and the operation

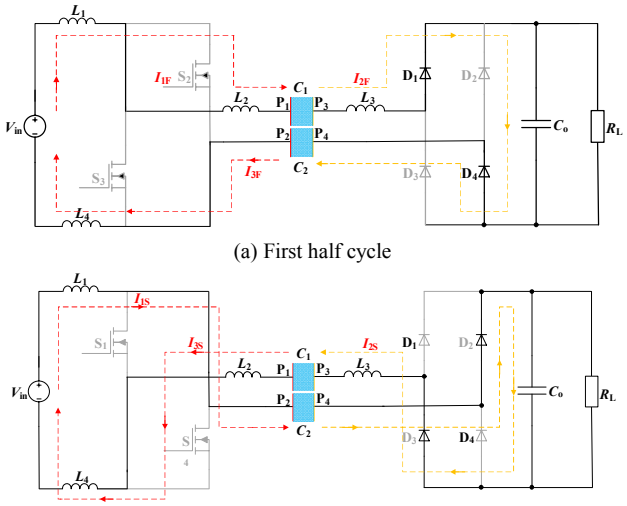

(a) First half cycle

(b) Second half cycle

Fig.4. Equivalent operating states of four-plate CPT system.

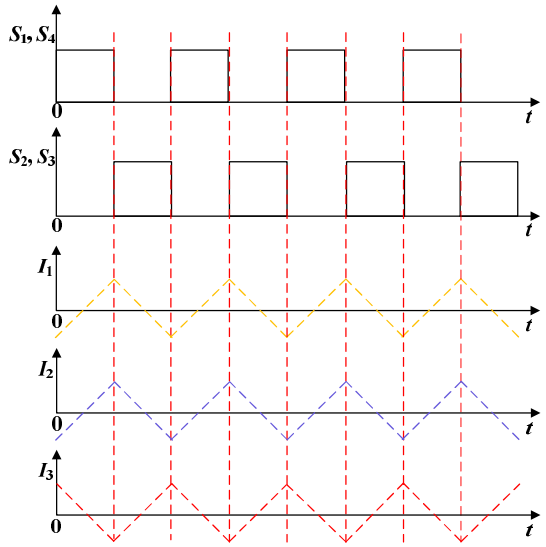

Fig.5. Operation timing waveforms of four-plate CPT system.

timing waveforms of the four-plate CPT system are respectively shown as Fig.4 and Fig. 5.

As shown in Fig.4 and Fig.5, in the first half cycle, the current I_{1F} flows from the power source to the inductor L_1, the inductor L_2 and the top coupling capacitor C_1. The current I_{2F} flows from top coupling capacitor C_1 and the inductor L_3 to the output filter capacitor C_o, load resistor R_L and the bottom coupling capacitor C_2. During the same period, the current I_{3F} flows from the bottom coupling capacitor C_2 to the inductor L_4 and the power source. As a result, a virtual closed-loop path is constructed. In the second half cycle, the current I_{1S} flows from the power source to the inductor L_1 and the bottom coupling capacitor C_2. The current I_{2S} flows from bottom coupling capacitor C_2 to the output filter capacitor C_o, load resistor R_L, the inductor L_3, and the top coupling capacitor C_1. During the same period, the current I_{3S} flows from the top coupling capacitor C_1, the inductor L_2 to the inductor L_4 and the power source. Then, another virtual closed-loop path is constructed. It can be seen from Fig.4, when S_1 and S_4 are ON, S_2 and S_3 are OFF, the currents I_1 and I_2 increase while the current I_3 decreases. When S_1 and S_4 are turned off, S_2 and S_3 are turned on, the currents I_1 and I_2 decrease while the current I_3 increases. The trend of the current I_2 is same to the current I_1. However, the current I_3 has the opposite trend to the currents I_1 and I_2. In one switching cycle, there are two closed-loop paths for the electrons flowing from the primary side to the secondary side. Then, the power could be wirelessly transferred from the power source side to the load side. In the seawater condition, the coupling capacitor model of four-plate CPT system could be drawn as Fig.6.

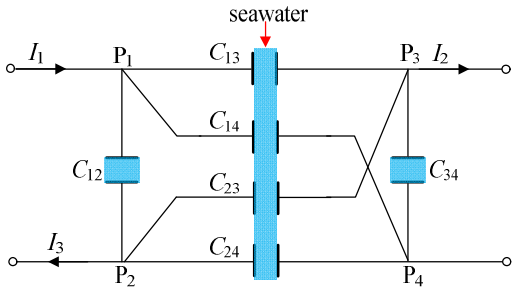

Fig.6. Coupling capacitor model in the seawater condition.

III. Theory Analysis

For the CPT system, it should build a closed-loop path for electrons. Based on the virtual electrons flow theory and the four-plate CPT system, in one switching cycle, the electrons are delivered two times through two different virtual closed-loop paths. As a result, the power will be transferred two times in one switching cycle from the power source to the load. The equivalent operating states of the four-plate CPT system based on the virtual electrons flow theory can be seen as Fig.4. According to Fig.4, in one switching cycle, the current I_1 has the same trend to the current I_2. The phase shift between the current I_3 and the currents I_1 and I_2 is 180°. For the sake of easy analysis, the internal resistance and the voltage of diodes are ignored. The internal resistance of the DC source is also not considered in the real calculation.

In the seawater condition, the permittivity of seawater determines the capacitance of the coupling capacitor. The permittivity of seawater, temperature, salinity and angular frequency of electromagnetic wave have a relationship as:

$$\varepsilon_{sea}(s,t,\omega)=\varepsilon_{\infty}(s,t)+\frac{\varepsilon_1(s,t)-\varepsilon_{\infty}(s,t)}{1-j\omega\tau(s,t)}-j\frac{\delta(s,t)}{\omega\varepsilon_0} \quad (1)$$

Where $\varepsilon_{\infty}(s,t)$ is the high-frequency seawater dielectric permittivity limit, $\varepsilon_0=8.854\times10^{-12}\,\mathrm{F/m}$ is the permittivity of free space, the angular frequency of electromagnetic wave $\omega=2\pi f$, f is the frequency of electromagnetic wave, $\varepsilon_1(s,t)$ is the static permittivity of seawater and $\delta(s,t)$ is the ionic conductivity of seawater.

The electric field intensity in the power transfer central channel could be written as:

$$E_D=\frac{E_o}{\varepsilon_{sea}(s,t,\omega)} \quad (2)$$

Considering the edge effects, with the seawater medium, the value of two coupling capacitor could be calculated as:

$$C = (1+2.343\times(\frac{D}{l})^{0.891})\times(\varepsilon_{sea}\times\frac{(l)^2}{D}) \tag{3}$$

Where l is the length of metal plate, D is the distance of one pair of plates, and ε_{sea} is the permittivity of seawater.

With the single-phase full-bridge inverter, the resonant voltage of the primary side could be derived as:

$$v_p = \frac{2\sqrt{2}}{p}v_{in} \tag{4}$$

On the other hand, with the single-phase full-bridge diode rectifier, the resonant voltage of the secondary side and the load voltage has a relationship as:

$$v_o = \frac{2\sqrt{2}}{\pi}v_s \tag{5}$$

There is an equivalent capacitor between every two metal plates, the six equivalent capacitors could be achieved in the coupling structure, as shown in Fig.5.

As shown in [33], based on the coupling capacitor structure model, the self-capacitance of primary side and self-capacitance of secondary side are expressed as follows:

$$C_p = C_{12} + \frac{(C_{13}+C_{14})\times(C_{23}+C_{24})}{C_{13}+C_{14}+C_{23}+C_{24}} \tag{6}$$

$$C_s = C_{34} + \frac{(C_{13}+C_{23})\times(C_{14}+C_{24})}{C_{13}+C_{14}+C_{23}+C_{24}} \tag{7}$$

and, the mutual capacitance could be written as:

$$C_M = \frac{C_{13}C_{24}-C_{14}C_{23}}{C_{13}+C_{14}+C_{23}+C_{24}} \tag{8}$$

The resonant compensation network is a simple LC network. As a result, the resonant frequency could be derived as:

$$f_s = \frac{1}{2\pi\sqrt{L_pC_p}} = \frac{1}{2\pi\sqrt{L_sC_s}} \tag{9}$$

Where L_p is the inductance of the equivalent inductor of the primary side resonant compensation network, and L_s is the inductance of the equivalent inductor of the secondary side resonant compensation network.

The angular frequency is written as:

$$\omega_s = 2\pi f_s = \frac{1}{\sqrt{L_pC_p}} = \frac{1}{\sqrt{L_sC_s}} \tag{10}$$

Considering the topology of the four-plate CPT system, the resonant voltage of the primary side v_p and the resonant voltage of the secondary side v_s have the relationship as:

$$v_s = \frac{j\omega C_pC_s}{C_M}v_p \tag{11}$$

In the first half-cycle, the equivalent circuit of the four-plate CPT system could be drawn as Fig.7. As shown in Fig. 7, the current flows through the virtual closed-loop path from the coupling capacitor C_1 to the coupling capacitor C_2. The isolation unit is the coupling capacitor C_1 and the coupling capacitor C_2. During the first half cycle, we set that the electrons flow in the forward direction. During this period, the current i_{1F} is equal to the current i_{2F}. It can be seen from Fig.7, the equivalent resistor of the forward path is consisted of the equivalent resistor of inductor L_1, the equivalent resistor of inductor L_2, the equivalent resistor of inductor L_3, the equivalent resistor of inductor L_4, the internal resistor of coupling capacitor C_1, the internal resistor of coupling capacitor C_2 and the resistor of the parallel connected output filter capacitor C_o and load resistor R_L.

Based on the KCL and KVL principles, the current i_{1F}, the current i_{2F} and the current i_{3F} in the first half cycle could be

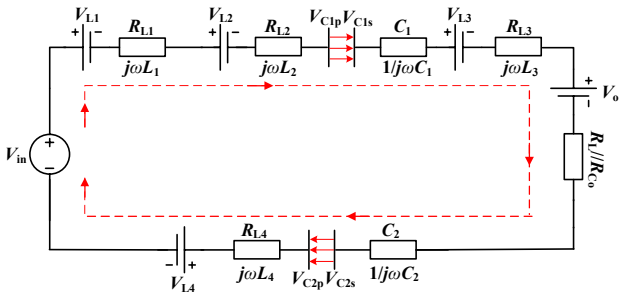

Fig.7. Equivalent circuit of four-plate CPT system in the first half cycle.

respectively derived as:

$$i_{1F} = \frac{(v_{in}-v_{L1}-v_{L2}-v_{C1p})}{j\omega_sL_1+j\omega_sL_2+1/j\omega_sC_1} \tag{12}$$

$$i_{2F} = \frac{(v_{C1s}-v_{L3}-v_o-v_{C2s})}{j\omega_sL_3+1/j\omega_sC_1+1/j\omega_sC_2+\dfrac{R_L}{1+j\omega_sC_oR_L}} \tag{13}$$

$$i_{3F} = -\left(\frac{v_{C2p}-v_{L4}+v_{in}}{j\omega_sL_4+1/j\omega_sC_2}\right) \tag{14}$$

Where v_{L1} is the voltage of the inductor L_1, v_{L2} is the voltage of the inductor L_2, v_{C1} is the voltage of the top coupling capacitor, v_{C2} is the voltage of the bottom coupling capacitor, v_{L3} is the voltage of the inductor L_3, v_{L4} is the voltage of the inductor L_4 and v_o is the load voltage.

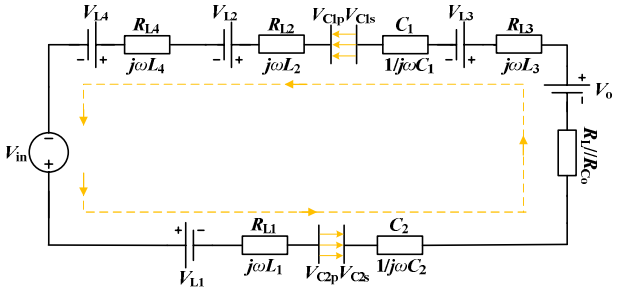

Fig.8. Equivalent circuit of four-plate CPT system in the second half cycle.

In the second half-cycle, the equivalent circuit of the four-plate CPT system could be drawn as Fig.8. It can be seen from Fig.8, the current i_{1S} is equal to the current i_{2S}. The current flows through the virtual closed-loop path from the coupling capacitor C_2 to the coupling capacitor C_1. The isolation unit is the coupling capacitor C_1 and the coupling

capacitor C_2. During the second half cycle, we set that the electrons flow in the inverse direction. As shown in Fig.8, the equivalent resistor of the inverse path is consisted of the equivalent resistor of inductor L_1, the equivalent resistor of inductor L_2, the equivalent resistor of inductor L_3, the equivalent resistor of inductor L_4, the internal resistor of coupling capacitor C_1, the internal resistor of coupling capacitor C_2 and the resistor of the parallel connected output filter capacitor C_o and load resistor R_L.

Based on the KCL and KVL principles, the current i_{1S}, the current i_{2S} and the current i_{3S} in the second half cycle could be respectively derived as:

$$i_{1S}=\frac{(v_{in}-v_{L1}-v_{C2p})}{j\omega_s L_1+1/j\omega_s C_2} \tag{15}$$

$$i_{2S}=\frac{(v_{C2s}+v_o-v_{L3}-v_{C1s})}{j\omega_s L_3+1/j\omega_s C_1+1/j\omega_s C_2+\dfrac{R_L}{1+j\omega_s C_o R_L}} \tag{16}$$

$$i_{3S}=-\left(\frac{(v_{C1p}-v_{L2}-v_{L4}+v_{in})}{j\omega_s L_2+j\omega_s L_4+1/j\omega_s C_1}\right) \tag{17}$$

The electric quantity which is transferred through the coupling capacitor in one switching cycle could be drawn as:

$$Q=\int_0^{0.5T_S} i_{1F}dt-\int_{0.5T_S}^{T_S} i_{1S}dt \tag{18}$$

Considering (11)-(16), in one switching cycle, the average load current could be derived as:

$$I_o=\frac{\int_0^{0.5T_S} i_{2F}\left(\dfrac{j\omega_s C_o R}{1+j\omega_s C_o R_L}\right)dt+\int_{0.5T_S}^{T_S} i_{2S}\left(\dfrac{j\omega_s C_o R}{1+j\omega_s C_o R_L}\right)dt}{T_S} \tag{19}$$

Considering (18), the output power can be expressed as:

$$P_o=(I_o)^2 R_L \tag{20}$$

IV. Experimental and Simulated Verification

To illustrate the viability of the virtual electrons periodic reciprocating flow theory for the four-plate CPT system in the undersea condition, the experimental setup is built as shown in Fig.9. A water tank is used to simulate the seawater environment. The parameters of the four-plate CPT system are shown as Table 1. The experimental temperature is 25℃. As shown in Table 1, the enhancement mode GaN-on-silicon transistor based full-bridge single-phase inverter and the full-bridge single-phase rectifier are adapted in the experiments. The experiments are conducted with the 400 mm distance between the transmitter metal plates and the receiver metal plates. The input voltage is set 100 V and the resonant frequency is set 500 kHz. The tested coupling capacitor is placed in the salty water condition with the salinity 35‰. The metal plates are covered by the waterproof plastic film. The simulation is conducted with PSIM and ANSYS Maxwell. The four-plate CPT system is controlled by the open-loop synchronous control method.

A. Simulated Verification

In order to measure the influence of meatal hull of AUV on electric fields, the simulation is conducted with the Ansys

TABLE I.
CIRCUIT PARAMETERS

Circuit parameters	Value
L_1	10 uH
L_2	75.10 uH
L_3	16.90 uH
L_4	10 uH
Input voltage	100 V
S_1, S_2, S_3, S_4	GS66508B, Simple gate drive requirements (0 V to 6 V), Transient tolerant gate drive (-20 V / +10 V), Very high switching frequency (> 10 MHz)
D_1, D_2, D_3, D_4	Fast Recovery Diode, VS-20CTH03STRL-M3, V_r=300 V, I_o=10 A, V_f=1.25V@10 A, t_{rr}=35 ns.
Switching frequency	500 kHz
C_p	1.35 nF
C_s	5.98 nF
Distance	10 mm~400 mm

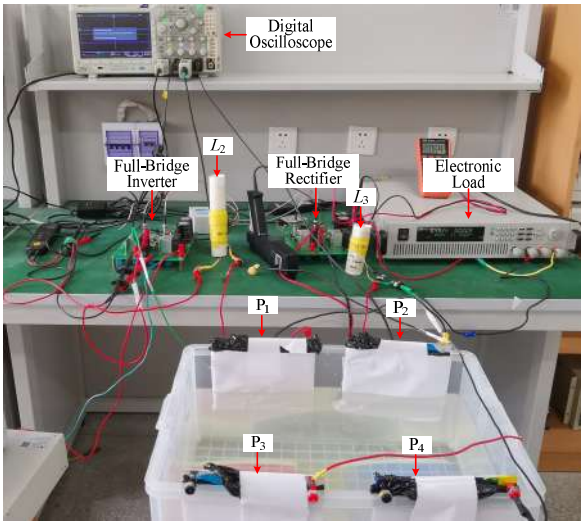

Fig.9. Experimental setup for the tested four-plate CPT system.

Maxwell software. The arc-shaped meatal plates are adapted to do the simulation work. The medium between the two AUVs is seawater with the 35‰ salinity. The size of the meatal plates is 170 mm×100 mm×5 mm. The radian is 15°. The distance between the two metal plates is 60 mm. The amplitude of alternating voltage injected on the two meatal plates is 220V. The simulated results are shown as Fig.10. It can be seen from Fig.10 (a), the electronic field is generated by the wireless power transfer system. When the two meatal plates of the CPT system placed between the two hulls of AUVs, the measured average electric field strength between the two metal plates is about 3142.9 V/m. As shown in Fig.10 (b), when one metal plate placed inside an AUV, the tested average electric field strength is about 3428.6 V/m. When the two meatal plates of the CPT system placed outside two hulls of AUVs as shown in Fig.10 (c), the measured electric field intensity between the two metal plates is about 3714.3 V/m. As a result, the meatal hull of AUV will have effect on the power transfer of CPT system. However, the impact is limited.

The simulation is conducted with the load resistance 100 Ω.

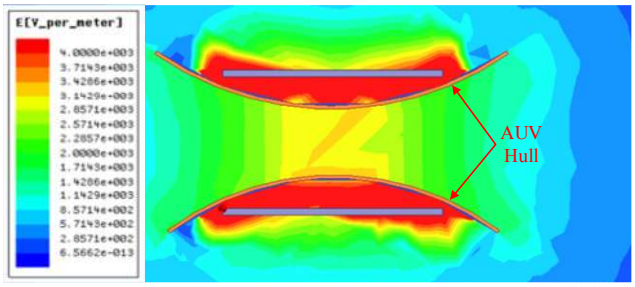

(a) Two meatal plates placed inside the AUVs

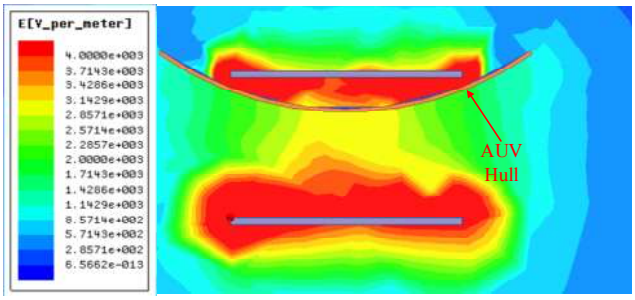

(b) One meatal plate placed inside the AUVs

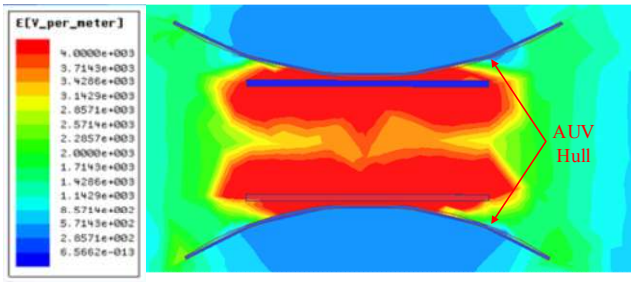

(c) Two meatal plates placed outside the AUVs

Fig.10. Simulated electronic fields.

The simulated results are shown as Fig.11. As shown in Fig. 11 (a), when switches S_1, S_2, S_3, and S_4 are turned on and off alternately, the current will be generated. The current I_1, I_2, and I_3 will flow periodically in one switching cycle. In the first half cycle, I_1 and I_2 will increase to the highest value. During the same period, I_3 will decrease to the lowest value. In the second half cycle, when I_1 and I_2 decrease, I_3 will increase. The maximum value of I_1, I_2 and I_3 is about 1 A and the minimum value of I_1, I_2 and I_3 is about -1 A. Based on the fore-mentioned discussion, in one switching cycle, the resonant current will have a forward path and an inverse path. As a result, in one switching cycle, there will be two virtual closed-loop paths for the electrons flowing from the power source to the load through the isolated coupling capacitors C_1 and C_2. The power is transferred two times from the primary side to the secondary side of the four-plate CPT system.

It can be seen from Figure 11 (b), with the input voltage 100 V, the measured load voltage is about 90 V. The input current is maintained stable without high spikes. The tested load current is about 0.99 A. As a result, the four-plate CPT system could work with the open-loop control method. It provides stable load voltage and load current.

The output voltage of the primary side full-bridge inverter and the input voltage of the secondary side full-bridge rectifier

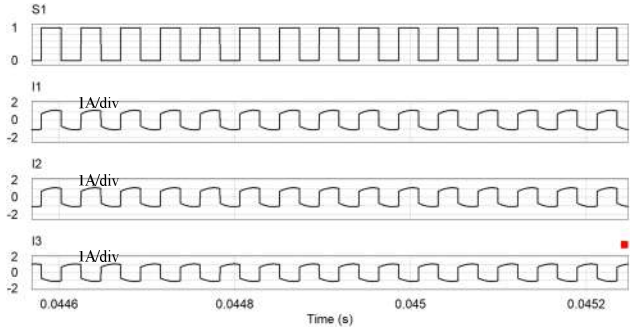

(a)

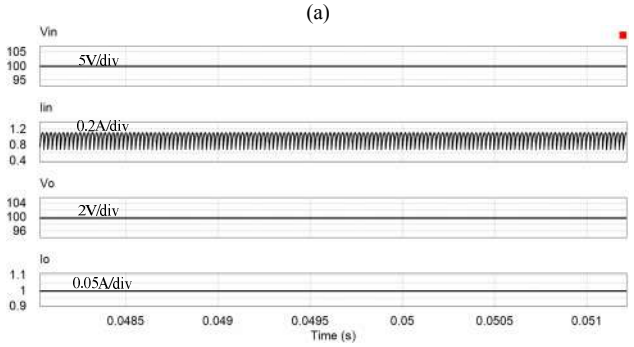

(b)

Fig.11 Simulated operation waveforms of four-plate CPT system.

are also measured in this paper. The simulated voltage waveforms of the four-plate CPT system are shown as Fig.12. It can be seen from Fig.12, the maximum value of the output voltage of the primary side full-bridge inverter and input voltage of the secondary side full-bridge rectifier is about 100 V.

This value is similar to the input voltage. The similar trend of these two voltages is achieved. With the four-plate CPT system, the power could be transferred with the low primary side resonant voltage and the secondary side resonant voltage.

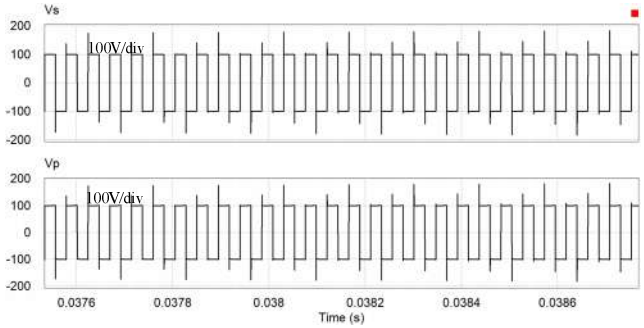

Fig.12. Simulated voltages of primary side and the secondary side of four-plate CPT system.

B. Experimental Verification

Experiments are conducted with the experimental prototype as shown in Fig.8. The experimental results are shown as Fig. 13 and Fig.14.

As shown in Fig.13 (a), in the salty water condition, the input current of the four-plate CPT system is continuous with the small current ripples. The load voltage is stable. As shown in Fig.12 (b), the voltage of the top coupling capacitor C_1 and the voltage of bottom coupling capacitor C_2 are also tested in this paper. As shown in Fig.13 (b), the voltage of coupling

capacitor C_1 has the opposite trend to the voltage of coupling capacitor C_2. It means that when the coupling capacitor C_1 is charged, the coupling capacitor C_2 discharges its energy, and vice versa. As a result, the coupling capacitor C_1 and the coupling capacitor C_2 will work complementarily with each other in one switching cycle. It has a good match with the theory analysis and the simulation results.

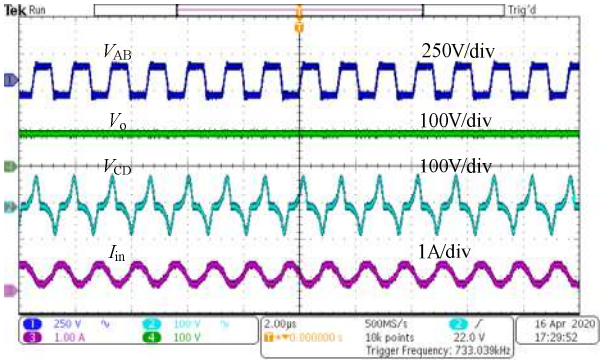

(a) voltages of primary side and the secondary side

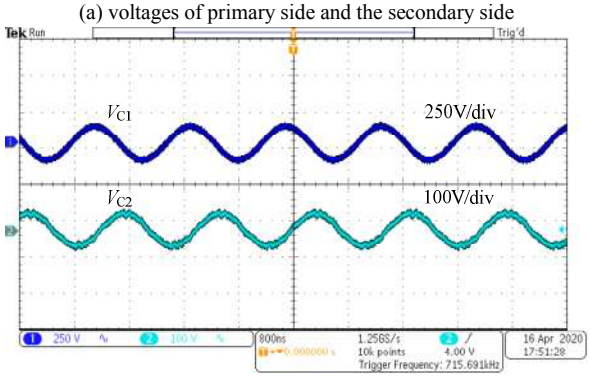

(b) voltages of coupling capacitors

Fig.13. Experimental operation waveforms of four-plate CPT system.

The resonant currents are also measured in the experiments. As shown in Fig.14, the current I_1 follows the voltage of the coupling capacitor C_1 and the current I_3 also follows the voltage of the coupling capacitor C_2. However, the current I_1 has the opposite trend to the current I_3. It also matches the theory analysis and the simulation results.

In the experiments, the efficiency is not high enough, with the power level 100 W and the distance 400 mm between the transmitter and the receiver, the maximum efficiency is about 50%. The reasons could be summarized as follows:

(a) The resonant compensation network is just an inductor, it is hard to maintain the resonant condition for the primary side and the secondary side of the CPT system at the same

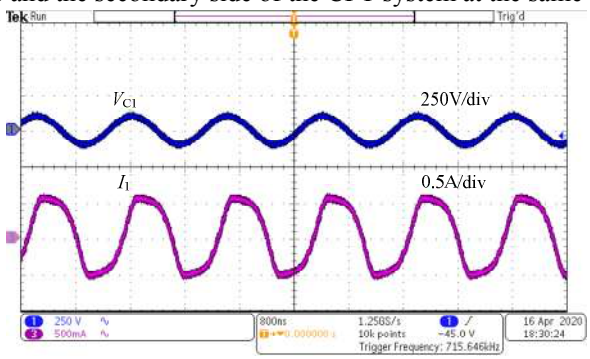

(a) voltage and current of coupling capacitor C_1

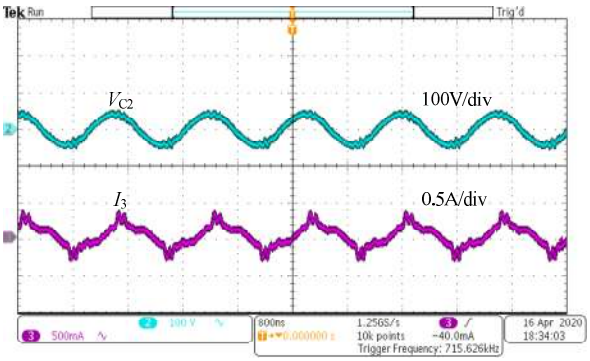

(b) voltage and current of coupling capacitor C_2.

Fig.14. Experimental voltage and current waveforms of coupling capacitors.

time. The optimized resonant compensation network will be built in the future work.

(b) The conductive feasibility of the salty water is still a challenge for the CPT system, the power loss theory analysis in the conductive water condition will be done in the future work.

(c) How to transfer the power with the long distance is still a key problem in the underwater applications especially for the undersea environment.

(d) As shown in the Fig.15 in the seawater condition, the coupling capacitor will have the dielectric resistance. The conductive seawater will generate the additional power loss. In the future work, the research work on the coupling capacitor structure in the seawater condition will be carried out to reduce the dielectric resistance power loss.

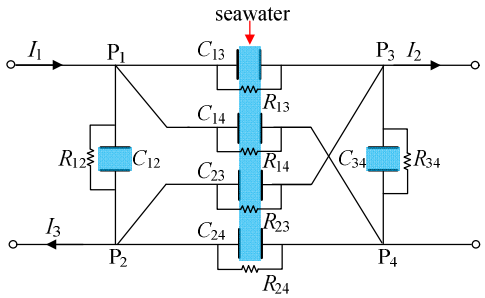

Fig.15. Equivalent circuit of the coupling capacitor structure in the seawater condition.

V. CONCLUSIONS

An undersea four-plate CPT system is built based on a virtual electrons periodic reciprocating flow theory. This theory is used for the wireless power transfer system which based on the electric fields. Two inductors are respectively connected to the coupling capacitors. The coupling capacitor is constructed by four metal plates. The dielectric between the four metal plates is the seawater. The electrons periodic reciprocating flow theory is verified by the simulation and experiments. The simulation is done with the PSIM and ANSYS Maxwell. In the experiments, a water tank with the 35‰ salinity is used to simulate the seawater condition. When the experiments are conducted, the four metal plates are placed in the salty water tank. The simulated and experimental

results show that the electrons flow in the two different closed-loop paths in one switching cycle and the power could be transferred two times in one switching cycle. The two coupling capacitors alternately receive energy and discharge the saved energy in one switching cycle. The tested four-plate CPT system could stably transfer the power in the salty water tank with the low resonant voltage. This paper could promote the future research work for the wireless power transfer system especially for the underwater wireless power transfer applications.

REFERENCES

[1] J. Xu, X. Li, H. Li, Z. Xie and Q. Ma, "Maximum Efficiency Tracking for Multi-Transmitter Multi-Receiver Wireless Power Transfer System on the Submerged Buoy," *IEEE Transactions on Industrial Electronics*, doi: 10.1109/TIE.2021.3063982.

[2] C. Anyapo and P. Intani. Wireless Power Transfer for Autonomous Underwater Vehicle. In Proceedings of 2020 IEEE PELS Workshop on Emerging Technologies: Wireless Power Transfer (WoW), Seoul, Korea (South), 15-19 Nov. 2020, pp. 246-249.

[3] K. Zhang, Y. Ma, Z. Yan, Z. Di, B. Song and A. P. Hu, "Eddy Current Loss and Detuning Effect of Seawater on Wireless Power Transfer," *IEEE Journal of Emerging and Selected Topics in Power Electronics*, vol. 8, no. 1, pp. 909-917, Mar. 2020.

[4] J. Zhou, P. Yao, Y. Chen, K. Guo, S. Hu and H. Sun, "Design Considerations for a Self-Latching Coupling Structure of Inductive Power Transfer for Autonomous Underwater Vehicle," *IEEE Transactions on Industry Applications*, vol. 57, no. 1, pp. 580-587, Jan.-Feb. 2021.

[5] I. R. Holgado, I. Martínez de Alegría, I. Kortabarria, J. Andreu and J. L. Martín. Wireless Power Transfer: Underwater loss analysis for different topologies and frequency values. In Proceedings of IECON 2020 The 46th Annual Conference of the IEEE Industrial Electronics Society, Singapore, 18-21 Oct. 2020, pp. 3942-3947.

[6] J. Kim et al.Analysis of Eddy Current Loss for Wireless Power Transfer in Conductive Medium Using Z-parameters Method. In Proceedings of 2020 IEEE Wireless Power Transfer Conference (WPTC), Seoul, Korea (South), 15-19 Nov. 2020, pp. 432-434.

[7] Z. Wang and S. Mirabbasi, "A Low-Voltage CMOS Rectifier With On-Chip Matching Network and a Magnetic Field Focused Antenna for Wirelessly Powered Medical Implants,"*IEEE Transactions on Biomedical Circuits and Systems*, vol. 13, no. 3, pp. 554-565, Jun.2019.

[8] Y. Jia, S. A. Mirbozorgi, P. Zhang, O. T. Inan, W. Li and M. Ghovanloo, "A Dual-Band Wireless Power Transmission System for Evaluating mm-Sized Implants," *IEEE Transactions on Biomedical Circuits and Systems*, vol. 13, no. 4, pp. 595-607, Aug. 2019.

[9] F. Yang, J. Fuh and P. Chen. A 13.56MHz Wireless Power Transfer System with Dual-Output Regulated Active Rectifier for Implantable Medical Devices. In Proceedings of 2018 IEEE 61st International Midwest Symposium on Circuits and Systems (MWSCAS), Windsor, ON, Canada, 5-8 Aug.2018, pp. 440-443.

[10] H. Mei, K. A. Thackston, R. A. Bercich, J. G. R. Jefferys and P. P. Irazoqui, "Cavity Resonator Wireless Power Transfer System for Freely Moving Animal Experiments," *IEEE Transactions on Biomedical Engineering*, vol. 64, no. 4, pp. 775-785, Apr.2017.

[11] Y. Lu, F. Mao and R. P. Martins. Bi-directional Battery-to-Battery Wireless Charging Enabled by Reconfigurable Wireless Power Transceivers (Invited Paper). In Proceedings of 2018 IEEE International Conference on Electron Devices and Solid State Circuits (EDSSC), Shenzhen, 6-8 Jun.2018, pp. 1-2.

[12] H. Hayashi et al.Effect of Body Materials on Transmission Efficiency and Resonant Frequency in Wirelessly Powered Personal Mobility Devices. In Proceedings of 2020 IEEE Wireless Power Transfer Conference (WPTC), Seoul, Korea (South),15-19 Nov. 2020, pp. 183-186.

[13] J. Song, M. Liu, N. Kang and C. Ma, "A Universal Optimal Drain–Source Voltage Tracking Scheme for Synchronous Resonant Rectifiers in Megahertz Wireless Power Transfer Applications," *IEEE Transactions on Power Electronics*, vol. 36, no. 5, pp. 5147-5156, May.2021.

[14] M. Huang, Y. Lu and R. P. Martins, "A Reconfigurable Bidirectional Wireless Power Transceiver for Battery-to-Battery Wireless Charging," *IEEE Transactions on Power Electronics*, vol. 34, no. 8, pp. 7745-7753, Aug. 2019.

[15] B. Regensburger, A. Kumar, S. Sinha and K. Afridi. High-Performance 13.56-MHz Large Air-Gap Capacitive Wireless Power Transfer System for Electric Vehicle Charging. In Proceedings of 2018 IEEE 19th Workshop on Control and Modeling for Power Electronics (COMPEL), Padua, 25-28 Jun.2018, pp. 1-4.

[16] J. Pries, V. P. N. Galigekere, O. C. Onar and G. Su, "A 50-kW Three-Phase Wireless Power Transfer System Using Bipolar Windings and Series Resonant Networks for Rotating Magnetic Fields," *IEEE Transactions on Power Electronics*, vol. 35, no. 5, pp. 4500-4517, May.2020.

[17] Y. Huang, C. Liu, Y. Zhou, Y. Xiao and S. Liu, "Power Allocation for Dynamic Dual-Pickup Wireless Charging System of Electric Vehicle," *IEEE Transactions on Magnetics*, vol. 55, no. 7, pp. 1-6, Jul. 2019.

[18] B. Regensburger, S. Sinha, A. Kumar, S. Maji and K. K. Afridi, "High-Performance Multi-MHz Capacitive Wireless Power Transfer System for EV Charging Utilizing Interleaved-Foil Coupled Inductors," *IEEE Journal of Emerging and Selected Topics in Power Electronics*, doi: 10.1109/JESTPE.2020.3030757.

[19] C. H. Lee, G. Jung, K. A. Hosani, B. Song, D. -k. Seo and D. Cho. Wireless Power Transfer System for an Autonomous Electric Vehicle. In Proceedings of 2020 IEEE Wireless Power Transfer Conference (WPTC), Seoul, Korea (South), 15-19 Nov. 2020, pp. 467-470.

[20] S. Ann and B. K. Lee, "Analysis of Impedance Tuning Control and Synchronous Switching Technique for a Semibridgeless Active Rectifier in Inductive Power Transfer Systems for Electric Vehicles," *IEEE Transactions on Power Electronics*, vol. 36, no. 8, pp. 8786-8798, Aug. 2021, doi: 10.1109/TPEL.2021.3049546.

[21] J. Zhou, B. Zhang, W. Xiao, D. Qiu and Y. Chen, "Nonlinear Parity-Time-Symmetric Model for Constant Efficiency Wireless Power Transfer: Application to a Drone-in-Flight Wireless Charging Platform," *IEEE Transactions on Industrial Electronics*, vol. 66, no. 5, pp. 4097-4107, May.2019.

[22] A. Iqbal, M. Al-Hasan, I. B. Mabrouk, A. Basir, M. Nedil and H. Yoo, "Biotelemetry and Wireless Powering of Biomedical Implants Using a Rectifier Integrated Self-Diplexing Implantable Antenna," *IEEE Transactions on Microwave Theory and Techniques*, vol. 69, no. 7, pp. 3438-3451, July 2021, doi: 10.1109/TMTT.2021.3065560.

[23] F. Lu, H. Zhang, H. Hofmann and C. Mi. A CLLC-compensated high power and large air-gap capacitive power transfer system for electric vehicle charging applications. In Proceedings of 2016 IEEE Applied Power Electronics Conference and Exposition (APEC), Long Beach, CA, 20-24 Mar.2016, pp. 1721-1725.

[24] F. Lu, H. Zhang, H. Hofmann, Y. Mei and C. Mi. A dynamic capacitive power transfer system with reduced power pulsation. In Proceedings of 2016 IEEE PELS Workshop on Emerging Technologies: Wireless Power Transfer (WoW), Knoxville, TN, 4-6 Oct. 2016, pp. 60-64.

[25] H. Zhang, F. Lu, H. Hofmann, W. Liu and C. C. Mi, "A Four-Plate Compact Capacitive Coupler Design and LCL-Compensated Topology for Capacitive Power Transfer in Electric Vehicle Charging Application," *IEEE Transactions on Power Electronics*, vol. 31, no. 12, pp. 8541-8551, Dec. 2016.

[26] H. Zhang, F. Lu, H. Hofmann, W. Liu and C. C. Mi, "Six-Plate Capacitive Coupler to Reduce Electric Field Emission in Large Air-Gap Capacitive Power Transfer," *IEEE Transactions on Power Electronics*, vol. 33, no. 1, pp. 665-675, Jan. 2018.

[27] F. Lu, H. Zhang, H. Hofmann and C. C. Mi, "An Inductive and Capacitive Integrated Coupler and Its LCL Compensation Circuit Design for Wireless Power Transfer," *IEEE Transactions on Industry Applications*, vol. 53, no. 5, pp. 4903-4913, Sept.-Oct. 2017.

[28] Hu Jie, Chen Lihua, Luo Bo, Shi Rui, and Mai Ruikun. Electric Field Coupled Power Transmission System with Dual Transmitting Terminals Based on Full-Capacitive Coupling Model. *Transactions of China Electrotechnical Society*, vol.34, no.17, pp:3542-3551, 2019.

[29] M. Tamura, Y. Naka, K. Murai and T. Nakata, "Design of a Capacitive Wireless Power Transfer System for Operation in Fresh Water," *IEEE*

Transactions on Microwave Theory and Techniques, vol. 66, no. 12, pp. 5873-5884, Dec. 2018.

[30] H. Zhang and F. Lu. Feasibility Study of the High-Power Underwater Capacitive Wireless Power Transfer for the Electric Ship Charging Application. In Proceedings of 2019 IEEE Electric Ship Technologies Symposium (ESTS), Washington, DC, USA, 14-16 Aug. 2019, pp. 231-235.

[31] L. Yang, L. Ma, J. Huang and Y. Fu. Characteristics of Undersea Capacitive Wireless Power Transfer System. In Proceedings of 2020 IEEE 9th International Power Electronics and Motion Control Conference (IPEMC2020-ECCE Asia), Nanjing, China,29 Nov.-2 Dec. 2020, pp. 2952-2955.

[32] L. Yang, M. Ju and B. Zhang, "Bidirectional Undersea Capacitive Wireless Power Transfer System," *IEEE Access*, vol. 7, pp. 121046-121054, 2019.

[33] E. Abramov, I. Zeltser and M. M. Peretz, "A network-based approach for modeling resonant capacitive wireless power transfer systems," *CPSS Transactions on Power Electronics and Applications*, vol. 4, no. 1, pp. 19-29, Mar.2019.

Lei Yang (S'15-M'17) was born in Henan, China, in 1986.He received the B.S degree in Electric and Information Engineering from Information Engineering University, Zhengzhou, China, in 2011, the M.S. degree in Signal and Information Processing (SIP) and the Ph.D. degree in Electrical Engineering from Northwestern Polytechnical University, Xi'an, Shaanxi, China, in April 2014 and in June 2017, respectively. He is currently working as an Assistant Professor at XI'AN University of Technology. From September 2014 to September 2016, he had been studied as a visiting student at University of California, Irvine, CA, USA.

His interest includes nonlinear control, switched-capacitor (SC) converter, DC-DC converter, power source of electrical vehicle, wireless power and data transfer system and renewable energy integration.

Yuanqi Zhang was born in Shaanxi, China, in 1999. He is currently studying in electrical engineering and automation of Xi'an University of technology. His main research direction in university is the control strategy of wireless power transmission system and bidirectional DC-DC converter.

Xiaojie Li was born in Shaanxi Province, China, in 1998.She received the B.S degree in Electrical Engineering and Automation from Xi'an University of Technology, Xi'an, Shaanxi Province, China, in June 2019, where she is currently pursuing M.S. degree. Her interests include the control strategy of wireless power transmission system, and bidirectional DC-DC converter.

Jiale Jian was born in Shaanxi, China, in 1999. In August 2018, he entered Xi'an University of Technology in Xi'an, Shaanxi, China, to study for B.S degree in Electrical Engineering and Automation. He is now a member of the research and development team of underwater wireless charging of Xi'an University of Technology. His main research direction in university is the control strategy of wireless power transmission system and bidirectional DC-DC converter.

Zhe Wang was born in Shaanxi in 2000. In August 2018, he entered Xi'an University of Technology in Xi'an , Shaanxi Province, China, to study for B.S degree in Electrical Engineering and Automation. He is now a member of the research and development team of underwater wireless charging of Xi'an University of Technology. His main research direction in university is the control strategy of wireless power transmission system and bidirectional DC-DC converter.

Jingjing Huang Jingjing Huang (Member, IEEE) received the B.S. degree from the Henan University of Science and Technology, Luoyang, China, in 2008, and the Ph.D. degree from Xi'an Jiaotong University, Xi'an, China, in 2014, both in electrical engineering.,From April 2014 to November 2016, she was a full-time Lecturer with the Xi'an University of Technology, Xi'an, China. From 2016 to 2019, she was a full-time Postdoctoral Research Fellow with Nanyang Technological University, Singapore. She is currently an Associate Professor with the School of Electronic and Information Engineering, Xi'an Jiaotong University. Her research interests include renewable energy systems, high-frequency transformer, hybrid ac/dc microgrid, and high-power converters.

Li Ma was born in Shaanxi Province, China, in 1993.He received the B.S degree in Electrical Engineering and Automation from Xi'an University of Technology, Xi'an, Shaanxi Province, China, in June 2016, where he is currently pursuing MS Degree at Xi'an University of Technology. His interests include wireless charging, DC-DC converter and Bidirectional OBC technology.

Xiangqian Tong was born in Shaanxi Province, China, in 1961. He received the B.S. degree in electrical engineering from the Shaanxi Institute of Technology, Han zhong, China, and the M.S. degree in electrical engineering from Xi'an University of Technology, Xi'an, China, in 1983 and 1989, respectively, and the Ph.D. degree in electrical engineering from Xi'an Jiaotong University, Xi'an, in 2006.He joined the Xi'an University of Technology in1989. Since 2002, he has been a Professor and the Academic Leader of Electrical Engineering at the Xi'an University of Technology.

His research interests include the application of power electronics in power systems and control of power quality, especially the power filter, static synchronous compensator, and high voltage direct current.